Research Square

Preprints are preliminary reports that have not undergone peer review.
They should not be considered conclusive, used to inform clinical practice,
or referenced by the media as validated information.

Time-series transcriptome analysis reveals the cascade mechanism of biological processes after perturbation of the MVA pathway in Salvia miltiorrhiza

Fang Liu
Chengdu University of Traditional Chinese Medicine School of Pharmacy
Nan Li
Chengdu University of Traditional Chinese Medicine School of Pharmacy
Zhu-Yun Yan
Chengdu University of Traditional Chinese Medicine School of Pharmacy
Xin Chen
chenxin@cdutcm.edu.cn

Chengdu University of Traditional Chinese Medicine School of Pharmacy

Research Article

Keywords: MVA pathway, HMGR inhibitor, Salvia miltiorrhiza Bunge., Time-series transcriptome, Gene regulatory network

Posted Date: June 5th, 2024

DOI: https://doi.org/10.21203/rs.3.rs-4465082/v1

License: This work is licensed under a Creative Commons Attribution 4.0 International License.
Read Full License

Additional Declarations: No competing interests reported.

Abstract

Background

Various biological processes are interconnected in plants. Transcription factors (TFs) often act as regulatory hubs to regulate plant growth and responses to stress by integrating various biological pathways. Despite extensive studies on TFs functions in various plant species, our understanding of the details of TFs regulation remains limited. In this study, clonal seedlings of *Salvia miltiorrhiza* were exposed to specific inhibitors for 12 hours. Time-series transcriptome data, sampled hourly, were used to construct co-expression networks and gene regulatory networks (GRNs). Transcriptome dynamic analysis was utilized to capture the gene expression dynamics of various biological processes and decipher the potential molecular mechanisms that regulate these processes.

Results

The perturbation results showed the growth and development processes of *S.miltiorrhiza* were primarily affected at the early stage, whereas stress response-related biological processes were mainly influenced at the later stage. And there was a correlation between the series of key differentially expressed genes in terpenoid biosynthesis pathways and the topological distribution of these pathways. Furthermore, the GRNs based on TFs indicate that TFs play a crucial role in connecting various biological processes. In the cytoplasmic lysate gene regulatory module, *Sm*WRKY48-*Sm*TCP*4*-*Sm*WRKY28 constituted a regulation hub regulating *S.miltiorrhiza* responses to perturbation of the MVA pathway. The regulation hub mediated various pathways, including pyruvate metabolism, glycolysis/gluconeogenesis, amino acid metabolism, and ubiquinone and other terpenoid-quinone biosynthesis.

Conclusion

Our findings suggest that perturbation of a key biological pathway in *S.miltiorrhiza* has time-dependent effects on other biological processes. And *Sm*WRKY48-*Sm*TCP4-*Sm*WRKY28 constitutes the regulatory hub in *S.miltiorrhiza* responses to perturbation of MVA pathway.

Background

Various biological processes are interconnected in plants. This connection is mediated through multiple molecular mechanisms. In contrast to other regulators like long non-coding RNAs (lncRNAs), microRNAs (miRNAs), and hormones, transcription factors (TFs) demonstrate a complex regulatory association with their target genes. Many TFs display a many-to-many regulatory pattern, enabling them to concurrently regulate multiple target genes involved in diverse biological processes [1]. This characteristic of TFs promotes the interconnectedness among various biological processes. TFs often act as the regulatory hubs regulating plant growth and responses to stress through integrating various pathways. For

instance, UB2/UB3/TSH4 acted as the signaling hubs regulating inflorescence development through integrating light and hormone signaling pathways in *Arabidopsis thaliana* [2].

The MYB-bHLH-WD40 regulatory complex controlled anthocyanidin biosynthesis in *Vaccinium corymbosum* fruit and color development [3]. The HSF, WRKY, and bZIP transcription factor families could regulate various biological processes in *Pinellia ternata* under shade conditions, including the accumulation of reactive oxygen species, light signals, and programmed cell death [4]. Transcription factor families such as MYB, bHLH, and NAC coordinated the interplay among the biosynthesis processes of secondary metabolites like flavonoids, caffeine, and theanine in tea trees [5].

Studies have shown that plants exhibit multiple temporal scales at different regulatory levels when faced with external stimuli. Transcriptional regulation can occur in minutes or hours [6]. Therefore, conducting a temporal transcriptome analysis over hours would be more beneficial for capturing dynamic events in gene transcriptional regulation, thus revealing the regulatory relationships between genes in a specific biological state. Time-sequence-based transcriptomes are preferred for constructing gene co-expression networks (GCNs) and gene regulatory networks (GRNs) [7]. For example, to investigate the molecular mechanism of salt stress tolerance in *Aquilegia vulgaris*, a time series transcriptome analysis was conducted. Samples were collected after exposure to NaCl treatment for 0, 12, 24, and 48 hours. The results showed that plant responses to salt stress involved cell wall composition and metabolism-related biological processes. Further analysis by constructing GRNs has revealed that the AP2, MYB, and bHLH transcription factor families might play crucial roles as key regulators in plant responses to salt stress [8]. To address the challenge of predicting causal relationships between TFs and their target genes, various algorithms have been developed to construct GRNs, including ARACNE (Algorithms for Reconstruction of Accurate Cellular Networks) [9], CLR (Context Likelihood of Relatedness) [10], GENIE3 (Gene Network Inference with Ensemble of Trees 3) [11], TIGRESS (Trustful Inference of Gene REgulation using Stability Selection) [12], and other methods. It has been discovered that no single method for GRN inference performs optimally across all datasets. Combinations of different method strategies often demonstrate robustness and superior performance in network inference, a phenomenon known as the “wisdom of the crowds” [13]. Specifically, bioNERO [14], an all-in-one R-package that encompasses all stages of the network analysis process, applies the “wisdom of the crowds” approach to constructing GRNs. It integrates three popular GRN inference algorithms - GENIE3, ARACNE, and CLR.

In plants, isoprenoids, also known as terpenes or terpenoids, are one of the most diverse organic compounds found in nature. They include primary products such as chlorophyll, carotenoids, ubiquinone, cytokines, gibberellin, oleuropein steroids, and abscisic acid, as well as numerous secondary metabolites with medicinal value, such as tanshinone, paclitaxel, artemisinin, and ginsenoside [15, 16]. Isoprenoids play a crucial role in growth, development, and stress responses. The mevalonic acid pathway (MVA) produces cytosolic isopentenyl diphosphate (IPP), while the methylerythritol pathway (MEP) generates IPP and its isomer dimethylallyl diphosphate (DMAPP) in plastids [17]. Changes in the expression of genes, the stability of proteins, and the activity of enzymes in either of these two pathways can affect a wide range of biological processes in plants [18]. For example, it was found that treating *Trigonella*

foenum-graecum with a specific inhibitor of HMGR (3-hydroxy-3-methyl glutaryl coenzyme A reductase) for 72 hours significantly inhibited root growth and resulted in a approximately 50% decrease in diosgenin content [19]. Overexpression of *Md*HMGR5 (from *Malus pumila*) in *Arabidopsis thaliana* enhanced the antioxidant stress capacity of the plant [20]. It suggests that when the MVA pathway is perturbed, multiple other biological processes will be affected.

Salvia miltiorrhiza is an important medicinal plant, with terpenoids and phenolic acids being its main medicinal components. Biological processes related to terpenoids have been extensively studied [21, 22]. This makes *S.miltiorrhiza* a valuable material for in-depth study of the role of the isoprenoid biosynthetic pathway in regulating plant metabolism and its relationship with other related pathways. In this study, we utilized lovastatin (LOV), a specific inhibitor of HMGR, to treat *S.miltiorrhiza* clonal seedlings. Subsequently, we conducted a dynamic transcriptome analysis. By constructing GCNs and GRNs, we have revealed the changing sequence of relevant biological processes and their underlying mechanisms following the perturbation of the MVA pathway.

Materials and methods

Plant material and growing conditions

Leaf explants were obtained from potted *S.miltiorrhiza* from the seed source of Zhongjiang County, Sichuan Province, China. The explants were then were used to induce callus formation and organogenesis [23]. Well-developed seedlings were transplanted into a series of MS [24] medium. Then the cultures were incubated in a growth chamber with a 14/10 hours (light/dark) photoperiod and a temperature of 24 ± 2℃.

Treatment of S.miltiorrhiza clonal seedlings with the inhibitor LOV

The activation of LOV and the preparation of stock solutions were performed as previously reported [25]. Clonal seedlings were transferred to MS medium containing the LOV final working solution concentrations of 10 μM [26]. The control samples were merely treated with LOV solvent. At different time intervals (2, 4, 6, 8, 10, and 12 hours) during the treatment (from 6:00 a.m. to 6:00 p.m.), the roots of clonal seedlings were harvested and stored at -80℃ for the time-series transcriptome sequencing and HMGR activity detection experiments. Clonal seedlings were transferred to MS medium containing the LOV final working solution concentrations of 0μM, 10μM, 50μM, 100μM, and 200μM. After 12 hours of treatment (at 6:00 p.m.), the roots of clonal seedlings were harvested and stored at -80℃ for the transcriptome sequencing. Three seedling roots were gathered per sample, with three biological replicates obtained for each time point and treatment concentration.

Total RNA extraction, library construction, sequencing and alignment

Total RNA was extracted from the roots using the MJZol Total RNA Extraction Kit (Majorbio Bio-Pharm Technology, Shanghai, China) following the manufacturer's instructions. Then, RNA quality was determined using the 5300 Bioanalyser (Agilent) and quantified with the ND-2000 (NanoDrop Technologies). Only high-quality RNA sample (OD260/280 = 1.8 ~ 2.2, OD260/230 ≥ 2.0, RQN ≥ 6.5, 28S:18S ≥ 1.0, > 1μg) was used to construct the sequencing library. RNA purification, reverse transcription, library construction, and sequencing were conducted at Shanghai Majorbio Bio-pharm Biotechnology Co., Ltd. (Shanghai, China) following the manufacturer's guidelines. The RNA-seq transcriptome library was prepared following Illumina® Stranded mRNA Prep Ligation (San Diego, CA). The sequencing library was prepared using the NovaSeq 6000 platform (PE150) and the NovaSeq Reagent Kit.

The raw paired-end reads were trimmed and quality-controlled using fastp [27] with default parameters. In this step, clean data was obtained by removing read segments containing artifacts and low-quality reads from the raw data. All subsequent analyses were based on high-quality, clean reads. Clean reads were separately aligned to *S.miltiorrhiza* reference genome in orientation mode using HISAT [28]. The reference genomes and gene annotations for chromosome-level genomes were downloaded directly from the website (https://ngdc.cncb.ac.cn/gwh/Assembly/10381/show) [29].

Differential expression analysis and functional enrichment

Gene expression was quantified using RNA-Seq via Expectation-Maximization (RSEM) [30] and then normalized by transcripts per kilobase per million mapped reads (TPM) values. Differential expression analysis was performed using the DESeq2 package [31]. To investigate the changes in the transcript abundance following LOV treatment, TPM values were utilized to calculate the gene expression level in the LOV-treated samples compared to the control samples. A gene was considered to be differentially expressed when it displayed an absolute value of log2 (fold change) ≥ 1 and an adjusted P-value < 0.5.

In addition, functional annotation of the differentially expressed genes (DEGs) was conducted using the Gene Ontology (GO) database (http://www.geneontology.org) and the Kyoto Encyclopedia of Genes and Genomes (KEGG) database (http://www.genome.jp/kegg/). Functional enrichment analysis, including GO and KEGG, was conducted to determine which DEGs were significantly enriched in various GO terms and metabolic pathways. GO functional enrichment and KEGG pathway analysis were conducted using Goatools and KOBAS software [32, 33].

HMGR activity assay

The roots of clonal seedlings were harvested after LOV treatment for 2, 4, 6, 8, 10, and 12 hours. Samples weighing 0.1 g were used for enzyme assays following the protocol outlined in the Plant HMGR ELISA KIT (Lunchangshuo Biotechnology, China).

Construction of GRNs

To obtain comprehensive gene functional information, the assembled transcriptome was annotated through BLAST searches against several databases, including Nr (Non-Redundant Protein Sequence Database) (https://www.ncbi.nlm.nih.gov/public/), eggNOG (Evolutionary Genealogy of Genes: Non-supervised Orthologous Groups) (http://eggnogdb.embl.de/#/app/home), Pfam (http://pfam.xfam.org/), GO (http://www.geneontology.org), KEGG (http://www.genome.jp/kegg/), and Swiss-Prot (http://web.expasy.org/docs/swiss-prot_guideline.html). TFs were screened based on the annotation information and classified according to PlantTFDB v5.0 (http://planttfdb_v4.cbi.pku.edu.cn/). TFs with normalized expression values (TPM) ≥ 1-fold change and an adjusted P-value < 0.5 were considered as differentially expressed TFs. Based on the GO annotation information, the DEGs annotated to the same cellular components, such as chloroplast, mitochondria, endoplasmic reticulum, Golgi apparatus, and cytoplasmic lysosome, were grouped into a gene set. GRNs were constructed based on differentially expressed TFs and DEGs in the gene set using bioNERO. Gephi [34] was used for visualizing GRNs and filtering the top 5 hub genes.

Construction of GCNs

The R package WGCNA (Weighted Gene Co-expression Network Analysis) [35] was used to construct GCNs. Firstly, the bioNERO R script was used to preprocess the gene expression data to remove the low expression data (TPM < 1). The outlier samples were then removed using the standardized connectivity method. Based on the topological overlap (TOM) dissimilarity, genes were clustered using the average-link hierarchical clustering method. The gene modules were determined using the dynamic cutting method. The correlation between the eigengene vector of the obtained module and the HMGR concentration of the sample was calculated using the function module-TraitCor. The module with the maximum correlation coefficient was chosen as the module significantly associated with HMGR concentration. The function expor-NetworkToCytascape was used to export the edge and node information of genes in each module. Finally, networks were visualized using Cytoscape v3.9.1 [36] and the top 10 hub genes in the networks were calculated using the Maximum Clique Centrality algorithm [37].

Quantitative real-time PCR verified selected genes

Total RNA was isolated using the Plant Total RNA Extraction kit (Foregene Biotech, Chengdu, China) and then treated with DNase I. First-strand cDNA was synthesized from the total RNA using the De-etiolated First-strand cDNA Synthesis Kit (Foregene Biotech, Chengdu, China). Quantitative real-time PCR (qRT-PCR) and data analyses were performed as previously described [38] and the 2^-ΔΔCT method [39] was used to calculate the relative abundance of selected genes. All primers were designed using Primer Premier 6 [40] and synthesized by Tsingke Biotech Co., Ltd. All primers used are listed in Supplementary Table S9.

Results

Differentially expressed genes(DEGs)analysis

At each sampling time point, genes with the normalized expression values (TPM) ≥ 2-fold change and an adjusted P-value < 0.5, compared with the control group, were considered as differentially expressed genes. Based on these criteria, a total of 748, 228, 239, 434, 887, and 1661 DEGs were identified after LOV treatment for 2, 4, 6, 8, 10, and 12 h, respectively. The sample treated with LOV for 12 hours showed the highest number of up-regulated genes (Fig. 1a). No genes have yet been found to be significantly differentially expressed in all six sampling time points. It has also been observed that when *S.miltiorrhiza* was first exposed to LOV, there was a period of rapid and significant changes in gene expression within a short timespan of 2 hours. Subsequently, the number of DEGs exhibited a tendency to gradually increase over time.

GO enrichment analysis of DEGs

The DEGs were analyzed by GO enrichment to characterize their functions at each sampling time points. The significantly enriched GO terms were identified based on the criterion of a P-value < 0.05 (Fig. 2a-f). The top 10 significantly enriched GO terms in the biological process (BP) category at each time point are presented in Supplementary Table S1. The results indicated that the BPs varied significantly at different time points. Among these BPs, the terms with the most DEGs at each time point were, in the following order: “carbohydrate metabolic process” (GO:0005975, 2 h, 46 DEGs), “terpene biosynthetic process” (GO:0016114, 4 h, 8 DEGs), “lipid X metabolic process” (GO:2001289, 6 h, 2 DEGs), “RNA processing” (GO:0006396, 8 h, 25 DEGs), “isoprenoid biosynthetic process” (GO:0008299, 10 h, 18 DEGs), “metabolic process” (GO:0008152, 12 h, 504 DEGs).

KEGG enrichment analysis of DEGs

KEGG is a knowledge base for the systematic analysis of gene functions, linking genomic information with higher-order functional information [41]. In this study, the DEGs were further analyzed using KEGG enrichment. The results showed that DEGs in all six sampling time points could be assigned to 26 pathways. Among these pathways, 24 pathways were related to metabolism. It indicated that the inhibitor primarily affected plant metabolism. After the 2 h, 10 h and 12 h of LOV treatment, “photosynthesis (map00195)” was significantly enriched. “Inositol phosphate metabolism (map00562)” was significantly enriched at 2 h and 4 h. “Biosynthesis of various plant secondary metabolites (map00999)” and “tyrosine metabolism (map00350)” were significantly enriched at 2 h and 12 h (Fig. 3).

Notably, DEGs enriched in various terpenoid biosynthesis-related processes at different time points. For instance, “monoterpenoid biosynthesis (map00902)” was significantly enriched in the samples treated with LOV for 2 h; “diterpenoid biosynthesis (map00904)” and “zeatin biosynthesis (map00908)” were significantly enriched at 4 h; “carotenoid biosynthesis (map00906)” was significantly enriched at 6 h; “sesquiterpenoid and triterpenoid biosynthesis (map00909)” and “terpenoid backbone biosynthesis (map00900)” were significantly enriched at 10 h (Fig. 3). This suggests that when plants are disturbed by LOV, the order of influence on terpenoid biosynthesis-related pathways is related to the topological

relationship among these pathways. Interestingly, the effect on “terpenoid backbone biosynthesis (map00900)” occurs at the late stage.

Analysis of differentially expressed TFs

TFs play crucial roles in regulating plant growth and development, as well as in responding to environmental stresses. In this experiment, a total of 79 differentially expressed TFs were identified in the samples treated with LOV, involving 18 of the 56 transcription factor families in *S.miltiorrhiza*, namely bHLH, bZIP, C2H2, HD-ZIP, HSF, MADS, MYB, NF-YA, AT-hook, GRAS, AP2/ERF, NZZ/ SPL, Nin-like, SRS, TCP, WRKY, ZF-HD, and BES1. The one with the highest number of differentially expressed TFs was the AP2/ERF family, comprising a total of 16 differentially expressed TFs (Fig. 4a).

The results also showed that the genes from 18 transcription factor families were expressed differentially at various time points. The sample with the most transcription factor families in differentially expressed genes was taken from the 12th hour (Fig. 4b). AT-hook and Nin-like families were predominantly differentially expressed in the early phase, while bHLH, HSF, AP2/ERF, and WRKY families were predominantly differentially expressed in the late phase. Some transcription factor families are expressed differentially at multiple time points. For example, the WOX family was differentially expressed at 2 h, 4 h, 10 h, and 12 h; the HSF family was differentially expressed at 2 h, 6 h, 8 h, and 12 h; the bZIP family was differentially expressed at 4 h, 8 h, 10 h, and 12 h. *Sm*WOX11-like, a member of the WOX family, was significantly differentially expressed in the samples treated with LOV for 4 h, 10 h, and 12 h. Details of the differentially expressed TFs at different time points are shown in Supplementary Table S2.

Analysis of GCNs

To investigate the co-expression dynamics of genes, a weighted gene co-expression network analysis was conducted. Total 116 co-expressed modules were identified. Among them, the turquoise module was the largest, containing 8,679 genes, while the steel blue and salmon modules showed a strong correlation with HMGR concentration (P-value < 0.05, Fig. 5a-c). The top 10 hub genes in the three modules were identified by analyzing nodes with centrality in the largest clusters (Table S3). Functional enrichment analysis of the three gene modules based on GO and KEGG was conducted to elucidate the underlying biological functions of these genes within their networks.

The genes of these three modules were enriched in various GO terms and metabolic pathways. The turquoise module was found to be significantly enriched in 944 GO terms (P-value < 0.05) (Fig. 6a). The KEGG enrichment analysis revealed that these genes can be categorized into 17 pathways (P-value < 0.05) (Fig. 7a), with 9 of these pathways belonging to the genetic information processing category. Analysis of the expression profiles of the top 10 hub genes in this module revealed that the peak expression of these genes occurred at hour 8 (Fig. S2a). It was indicated that the genes involved in genetic information processing biological processes were actively expressed after inhibitor treatment for 8 hours. A total of 623 and 331 GO terms were significantly enriched in the steel blue and salmon modules (P-value < 0.05) (Fig. 6b-c). The enriched terms indicated that the steel blue and salmon modules were primarily associated with macromolecular biosynthesis and sugar metabolism. The KEGG

enrichment analysis revealed that these genes were assigned to 27 and 24 pathways (P-value < 0.05). Among them, 14 and 17 pathways are associated with energy metabolism (Fig. 7b-c). This indicates that many pathways related to energy metabolism responded positively to changes in HMGR activity. Analysis of the expression profiles of the top 10 hub genes in the steel blue and salmon modules revealed that the peak expression of these genes occurred at hour 10 (Fig. S2b-c). The results indicated that the genes in the energy metabolism pathway were actively expressed after 10 hours of inhibitor treatment.

Analysis of GRNs

Unlike the GCN, the GRN can be used to study the regulatory relationships between genes. It is known that gene regulation occurs in the nucleus, and the proteins encoded by these genes play roles in various subcellular locations. GO organizes biological knowledge about cell components hierarchically. This makes GRNs analysis not only interpretable mechanistically but also provides new mechanistic insights [42]. Therefore, in constructing GRNs, DEGs were first classified into five gene sets based on GO subcellular localization annotations. The GO terms of these five gene sets are related to “chloroplast”, “mitochondria”, “endoplasmic reticulum”, “Golgi apparatus”, and “cytoplasmic lysosomal”. Five GRNs were constructed based on these five gene sets and differentially expressed TFs (Fig. 8, Fig. S4), and the top 5 hub genes in each network were identified (Table S5).

The target genes of these specific regulators are involved in various biological pathways (Table S6). For example, in the chloroplast gene regulatory module, *Sm*WRKY48 targeted genes involved in fatty acid biosynthesis, pyruvate metabolism, photosynthesis, arginine biosynthesis, and other pathways. In the mitochondrial gene regulatory module, the target genes of *Sm*AGL16 were involved in various pathways, such as nicotinate and nicotinamide metabolism, pantothenate and CoA biosynthesis, amino acid metabolism and degradation, aminoacyl-tRNA biosynthesis, folate biosynthesis, and other biological processes. In the cytoplasmic lysate gene regulatory module, *Sm*WRKY28 targeted genes involved in glutathione metabolism, pyruvate metabolism, cysteine and methionine metabolism, and glycolysis/gluconeogenesis pathways. Similarly, in *A.thaliana*, the homologous genes of these TFs also exhibit the behavior of targeting genes involved in various biological processes. For example, *At*WRKY48, a homologous gene of *Sm*WRKY48, targeted *At*ASP, *At*IAA2, and *At*DLDG1 in *A.thaliana* acclimation to a combination of high light and heat stress; *At*AGL16, a homologous gene of *Sm*AGL16, regulated the expression of *At*HKT1;1, *At*HsfA6a, and *At*MYB102 in *A.thaliana* salt stress response; *At*WRKY28, a homologous gene of *Sm*WRKY28, targeted genes in the salicylic acid and jasmonic acid/ethylene-dependent defense pathways in *A.thaliana* streptococcus bacteriophage and oxalic acid stress response [43–45].

TFs, as a regulatory center, regulate *S.miltiorrhiza* responses to MVA pathway interference by integrating various biological pathways. In the cytoplasmic lysate gene regulatory network, *Sm*WRKY48-*Sm*TCP4-*Sm*WRKY28 worked as a regulation hub to integrate various biological processes, including pyruvate metabolism, glycolysis/gluconeogenesis, amino acid metabolism, and ubiquinone and other terpenoid-quinone biosynthesis (Fig. 8). In order to further verify whether the identified TFs have a specific

response to LOV, the expression profiles of TFs were analyzed after treatment with different concentrations of LOV (Fig. 9). It was found that the expression of *Sm*WRKY28 and *Sm*WRKY48 fluctuated greatly, while there was no significant change in *Sm*TCP4 expression.

In this study, it was relatively common that a target gene was regulated by several transcription factors. For example, in the chloroplast gene regulatory module, the gene *Sm*PSBR, which is involved in the photosynthesis pathway, was simultaneously targeted by the transcription factors *Sm*CPRF1, *Sm*ABR1, and *Sm*WRKY48. In the mitochondrial gene regulatory module, the gene *Sm*PDL2, which is involved in the folate biosynthesis pathway, was targeted by the transcription factors *Sm*WRKY48, *Sm*AGL16, and *Sm*ERF010.

Validation of RNA-Seq sequencing data by qPCR analysis

To validate the reliability of transcriptome sequencing data, 10 genes were selected for expression correlation analysis: DXS, HMGS, HMGR, IDI, KSL, GA3, CPRF1, TCP4, WRKY40, and WRKY48. The results indicate that the majority of the selected genes displayed expression patterns consistent with the results of transcriptome sequencing, affirming the credibility of our transcriptome data (Fig. S3).

Discussion

Perturbation of essential biological pathways in plants leads to consequences on both their primary and secondary metabolic pathways. In the current study, by perturbing the MVA pathway in *S.miltiorrhiza*, we observed significant differential expression of genes involved in plant primary metabolic processes, such as energy metabolism, carbohydrate metabolism, amino acid metabolism, and lipid compound metabolism. Moreover, genes associated with plant secondary metabolic processes, including terpene and polyketide metabolism, also showed significant differential expression (Fig. 3). The results of the GCNs analysis indicated that genes in the steel blue module and salmon module exhibit significant enrichment for biological processes associated with primary metabolism, such as carbon fixation in photosynthetic organisms, pyruvate metabolism, and glycolysis/gluconeogenesis (Fig. 7). Multiple established studies have also demonstrated that perturbing a specific biological pathway in plants can have implications for several other related biological processes. For example, in *A.thaliana*, interference with the histidine biosynthesis pathway not only blocked histidine biosynthesis but also impacted aromatic amino acids (such as histidine, lysine, and purine) and the tryptophan biosynthesis pathway [46]. After treating pear fruit (cv. "Blanquilla") with LOV, various biological processes were influenced, including the metabolism of ascorbic acid, the biosynthesis of phenolic compounds, and lipid biosynthesis [47]. When the photosynthetic biological processes of *Oryza sativa* were disturbed, not only was the photosynthetic pathway affected, but also oxidation/reduction-related biological processes were significantly impacted [48]. Overexpression of APR2, a gene in the sulfate reduction assimilation pathway in *A.thaliana*, promoted the biosynthesis of glutathione and phytochelatins [49]. Perturbation of the jasmonic acid biosynthesis pathway in *Oryza sativa* revealed that the processes of sugar metabolism, cell wall biosynthesis, and diurnal flowering time were impacted [50].

Perturbation of the MVA pathway in *S.miltiorrhiza* affected several biological processes at different time points. In the early stage (2–6 h), it mainly affected biological processes related to plant growth and development, such as the cell cycle, morphogenesis, and photosynthesis. However, in the late period (8–12 h), it primarily impacted biological processes associated with stress response, including systemic acquired resistance, osmotic stress, water stress, oxidative stress, and cold stress (Fig. 2). Time-dependent changes in transcript expression profiles have also been observed in other plants. For instance, the functional analysis of genes responding at different time points during progressive drought in *A.thaliana* revealed that early DEGs were associated with biological processes such as carbohydrate and glycoside biosynthesis, while late DEGs were involved in flavonoid and pigment biosynthesis [51]. The results of a time-series transcriptome analysis of *Populus* in response to salt stress revealed that it primarily impacted the plant photosynthesis process in the early stage. Subsequently, it triggered the stress resistance response, activated hormone signaling pathways, and influenced flavonoid biosynthesis and metabolism-related processes in the middle and late stages [52]. After 2 hours of cold treatment in *Ricinus communis*, the DEGs were primarily associated with plant pathogen interactions and autophagy regulation processes. Subsequently, the DEGs were linked to plant circadian rhythms and hormone signaling processes following cold treatment for 6 and 8 hours [53]. Salt stress treatment was observed to primarily impact biological processes associated with plant hormone metabolism during the early stage of stress (6 hours) and photosynthesis-related biological processes during the later stage (7 days) in *Vitis vinifera* [54].

The changes in biological processes resulting from LOV treatment, occurring at various time intervals, are linked to the topological arrangement of these pathways in the KEGG diagram. This investigation demonstrated that DEGs at different time points were connected to specific terpenoid biosynthesis pathways. For instance, the DEGs were associated with specific biological processes at different time points: monoterpenoid biosynthesis at 2 h, diterpenoid biosynthesis and zeatin biosynthesis at 4 h, carotenoid biosynthesis at 6 h, and terpenoid backbone biosynthesis as well as sesquiterpenoid and triterpenoid biosynthesis at 10 h (Table S11). By perturbing the MVA pathway, the biosynthesis pathways for monoterpenoids, diterpenoids, zeatin, and carotenoids, located downstream of the terpenoid backbone biosynthesis pathway, were notably influenced at the early stage. Subsequently, genes in the MVA pathway and MEP pathway, which are situated upstream of the terpenoid backbone biosynthesis pathway, were significantly affected at a later time point (Fig. 10). It has been reported that the inhibition of HMGR activity using LOV led to decreased expression levels of genes downstream of the terpenoid backbone biosynthesis pathway, including MK, PMK, DPMD, SLS, and STR [55]. Our study reveals the sequence of the affected biosynthetic pathways when the MVA pathway in *S.miltiorrhiza* was perturbated by an inhibitor. It is closely associated with the topological relationships between these biosynthetic pathways.

TFs often act as the regulatory hubs regulating plant responses to stress through mediating synergistic interactions among distinct biological processes in plants. The constructed GRNs in this study demonstrated that TFs targeted genes from multiple biological pathways. In this study, a transcription factor combination, *Sm*WRKY48-*Sm*TCP4-*Sm*WRKY28, was found in the cytoplasmic lysate gene

regulatory network. *Sm*WRKY48-*Sm*TCP4-*Sm*WRKY28 targeted genes involved in pyruvate metabolism, glycolysis/gluconeogenesis, amino acid metabolism, and ubiquinone and other terpenoid-quinone biosynthesis (Fig. 8). Research has also demonstrated that WRKY genes can regulate plant stress tolerance by acting in conjunction with other TFs. For example, *At*WRKY18, *At*WRKY40 and *At*WRKY60 TFs form a highly interacting regulatory network that modulates gene expression in *A.thaliana* responses to abscisic acid and abiotic stress [56]. *At*WRKY70 and *At*WRKY54 co-operate as negative regulators of the osmotic stress response in *A.thaliana* [57]. *Pe*HSF-*Pe*WRKY1 regulated the K^+/Na^+ homeostasis under high-salinity conditions in *Populus euphratica* [58].Therefore, we can find that the dynamic combination of transcription factors endows plants with robustness to adapt to the environment under different circumstances.

Conclusion

Our findings suggest that perturbation of a key biological pathway in *S.miltiorrhiza* has time-dependent effects on other biological processes. In general, the growth and development processes of *S.miltiorrhiza* are primarily affected at the early stage, whereas stress response-related biological processes are mainly influenced at the later stage. Additionally, pathways, located downstream of the terpenoid backbone biosynthesis pathway, are predominantly affected at the early stage. The MVA and MEP pathways are impacted at the later stage. This suggests that the order of the affected biosynthetic pathways is associated with the topological distribution of these biological pathways. The GRNs based on TFs indicated that *Sm*WRKY48-*Sm*TCP4-*Sm*WRKY28 worked as a regulation hub to integrate synergistic interactions among distinct biological processes in *S.miltiorrhiza.* These findings provide insights for a deeper understanding of the molecular mechanisms through which various biological processes synergistically interact.

Declarations

Ethics declarations

Not applicable.

Consent for publication

Not applicable.

Data availability

All data supporting the findings of this study are included in this manuscript and its supplementary files or further materials can be obtain from the corresponding author upon request. The transcriptome sequencing data that support the findings of this study have been deposited in NCBI Sequence Read Archive with the accession code PRJNA1111691 and PRJNA1112563. Source data are provided with this paper.

Conflict of interest

The authors declare no competing financial interests.

Funding

This study was funded by the National Natural Science Foundation of China (82373984).

Natural Science Foundation of China: 82373984.

Authors' contributions

All authors contributed to the study conception and design. **LF** conceived, designed, performed the experiments and data analysis, and wrote the manuscript. **LN** contributed to data analysis and manuscript writing. **YZY** conceived and designed experiments, wrote or reviewed drafts of papers. **CX** conceived and designed experiments, wrote or reviewed drafts of papers. All authors contributed to the article and approved the submitted version.

Authors' information

School of Pharmacy, Chengdu University of Traditional Chinese Medicine, Chengdu, Sichuan, China

Fang Liu, Nan Li, Zhu-Yun Yan & Xin Chen

Corresponding author

Xin Chen, chenxin@cdutcm.edu.cn

Acknowledgements

Not applicable.

References

1. Shen-Orr SS, Milo R, Mangan S, Alon U: **Network motifs in the transcriptional regulation network of Escherichia coli**. *Nature Genetics* 2002, **31**(1):64-68.
2. Kong D, Li C, Xue W, Wei H, Ding H, Hu G, Zhang X, Zhang G, Zou T, Xian Y *et al*: **UB2/UB3/TSH4-anchored transcriptional networks regulate early maize inflorescence development in response to simulated shade**. *Plant Cell* 2023, **35**(2):717-737.
3. Zhao M, Li J, Zhu L, Chang P, Li L, Zhang L: **Identification and Characterization of MYB-bHLH-WD40 Regulatory Complex Members Controlling Anthocyanidin Biosynthesis in Blueberry Fruits Development**. *Genes (Basel)* 2019, **10**(7).
4. Yang J, Cui W, You Q, Liu M, Liu X, Zhao F, Zhu Y, Duan Y, Xue T, Xue J: **Transcriptome Analysis Reveals Long Non-Coding RNAs Involved in Shade-Induced Growth Promotion in Pinellia ternata**.

FBL 2023, **28**(9).

5. Li C-F, Zhu Y, Yu Y, Zhao Q-Y, Wang S-J, Wang X-C, Yao M-Z, Luo D, Li X, Chen L *et al*: **Global transcriptome and gene regulation network for secondary metabolite biosynthesis of tea plant (Camellia sinensis)**. *BMC Genomics* 2015, **16**(1):560.
6. Li Y, Varala K, Coruzzi GM: **From milliseconds to lifetimes: tracking the dynamic behavior of transcription factors in gene networks**. *Trends in Genetics* 2015, **31**(9):509-515.
7. Alvarez JM, Brooks MD, Swift J, Coruzzi GM: **Time-Based Systems Biology Approaches to Capture and Model Dynamic Gene Regulatory Networks**. *Annual Review of Plant Biology* 2021, **72**(1):105-131.
8. Bai Y, Yu H, Chen L, Meng Y, Ma Y, Wang D, Qian Y, Zhang D, Feng X, Zhou Y: **Time-Course Transcriptome Analysis of Aquilegia vulgaris Root Reveals the Cell Wall’s Roles in Salinity Tolerance**. *International Journal of Molecular Sciences* 2023, **24**(22):16450.
9. Margolin AA, Nemenman I, Basso K, Wiggins C, Stolovitzky G, Favera RD, Califano A: **ARACNE: An Algorithm for the Reconstruction of Gene Regulatory Networks in a Mammalian Cellular Context**. *BMC Bioinformatics* 2006, **7**(1):S7.
10. Faith JJ, Hayete B, Thaden JT, Mogno I, Wierzbowski J, Cottarel G, Kasif S, Collins JJ, Gardner TS: **Large-scale mapping and validation of Escherichia coli transcriptional regulation from a compendium of expression profiles**. *PLoS Biol* 2007, **5**(1):e8.
11. Huynh-Thu VA, Irrthum A, Wehenkel L, Geurts P: **Inferring regulatory networks from expression data using tree-based methods**. *PLoS One* 2010, **5**(9).
12. Haury AC, Mordelet F, Vera-Licona P, Vert JP: **TIGRESS: Trustful Inference of Gene REgulation using Stability Selection**. *BMC Syst Biol* 2012, **6**:145.
13. Marbach D, Costello JC, Küffner R, Vega NM, Prill RJ, Camacho DM, Allison KR, Aderhold A, Allison KR, Bonneau R *et al*: **Wisdom of crowds for robust gene network inference**. *Nature Methods* 2012, **9**(8):796-804.
14. Almeida-Silva F, Venancio TM: **BioNERO: an all-in-one R/Bioconductor package for comprehensive and easy biological network reconstruction**. *Funct Integr Genomics* 2022, **22**(1):131-136.
15. Pichersky E, Raguso RA: **Why do plants produce so many terpenoid compounds?** *New Phytologist* 2018, **220**(3):692-702.
16. Krause T, Wiesinger P, González-Cabanelas D, Lackus N, Köllner TG, Klüpfel T, Williams J, Rohwer J, Gershenzon J, Schmidt A: **HDR, the last enzyme in the MEP pathway, differently regulates isoprenoid biosynthesis in two woody plants**. *Plant Physiology* 2023, **192**(2):767-788.
17. Rohmer M, Rohmer M: **The discovery of a mevalonate-independent pathway for isoprenoid biosynthesis in bacteria, algae and higher plants†**. *Natural Product Reports* 1999, **16**(5):565-574.
18. Cho S-H, Tóth K, Kim D, Vo PH, Lin C-H, Handakumbura PP, Ubach AR, Evans S, Paša-Tolić L, Stacey G: **Activation of the plant mevalonate pathway by extracellular ATP**. *Nature Communications* 2022, **13**(1).

19. Cao L, Zhou Z, Sun J, Li C, Zhang Y: **Altering Sterol Composition Implied That Cholesterol Is Not Physiologically Associated With Diosgenin Biosynthesis in Trigonella foenum-graecum**. *Frontiers in Plant Science* 2021, **12**.
20. Zhang M, Liu H, Wang Q, Liu S, Zhang Y: **The 3-hydroxy-3-methylglutaryl-coenzyme A reductase 5 gene from Malus domestica enhances oxidative stress tolerance in Arabidopsis thaliana**. *Plant Physiology and Biochemistry* 2020, **146**:269-277.
21. Gao W, Sun HX, Xiao H, Cui G, Hillwig ML, Jackson A, Wang X, Shen Y, Zhao N, Zhang L *et al*: **Combining metabolomics and transcriptomics to characterize tanshinone biosynthesis in Salvia miltiorrhiza**. *BMC Genomics* 2014, **15**:73.
22. Lu LL, Zhang YX, Yang YF: **Integrative transcriptomic and metabolomic analyses unveil tanshinone biosynthesis in Salvia miltiorrhiza root under N starvation stress**. *PLoS One* 2022, **17**(8):e0273495.
23. Tsai K-L, Chen EG, Chen J-T: **Thidiazuron-induced efficient propagation of Salvia miltiorrhiza through in vitro organogenesis and medicinal constituents of regenerated plants**. *Acta Physiologiae Plantarum* 2015, **38**(1):29.
24. Murashige T, Skoog FK: **A revised medium for rapid growth and bio assays with tobacco tissue cultures**. *Physiologia Plantarum* 1962, **15**:473-497.
25. Hagen C, Grunewald K: **Fosmidomycin as an inhibitor of the non-mevalonate terpenoid pathway depresses synthesis of secondary carotenoids in flagellates of the green alga Haematococcus pluvialis**. *JOURNAL OF APPLIED BOTANY-ANGEWANDTE BOTANIK* 2000, **74**(3-4):137-140.
26. Blazquez MA, Yang D, Du X, Liang X, Han R, Liang Z, Liu Y, Liu F, Zhao J: **Different Roles of the Mevalonate and Methylerythritol Phosphate Pathways in Cell Growth and Tanshinone Production of Salvia miltiorrhiza Hairy Roots**. *PLoS ONE* 2012, **7**(11).
27. Chen S, Zhou Y, Chen Y, Gu J: **fastp: an ultra-fast all-in-one FASTQ preprocessor**. *Bioinformatics* 2018, **34**(17):i884-i890.
28. Kim D, Langmead B, Salzberg SL: **HISAT: a fast spliced aligner with low memory requirements**. *Nat Methods* 2015, **12**(4):357-360.
29. Song Z, Lin C, Xing P, Fen Y, Jin H, Zhou C, Gu YQ, Wang J, Li X: **A high-quality reference genome sequence of Salvia miltiorrhiza provides insights into tanshinone synthesis in its red rhizomes**. *Plant Genome* 2020, **13**(3):e20041.
30. Li B, Dewey CN: **RSEM: accurate transcript quantification from RNA-Seq data with or without a reference genome**. *BMC Bioinformatics* 2011, **12**:323.
31. Love MI, Huber W, Anders S: **Moderated estimation of fold change and dispersion for RNA-seq data with DESeq2**. *Genome Biol* 2014, **15**(12):550.
32. Young MD, Wakefield MJ, Smyth GK, Oshlack A: **Gene ontology analysis for RNA-seq: accounting for selection bias**. *Genome Biol* 2010, **11**(2):R14.
33. Kanehisa M, Araki M, Goto S, Hattori M, Hirakawa M, Itoh M, Katayama T, Kawashima S, Okuda S, Tokimatsu T *et al*: **KEGG for linking genomes to life and the environment**. *Nucleic Acids Res* 2008, **36**(Database issue):D480-484.

34. Bastian M, Heymann S, Jacomy M: **Gephi: An Open Source Software for Exploring and Manipulating Networks**. 2009.
35. Langfelder P, Horvath S: **WGCNA: an R package for weighted correlation network analysis**. *BMC Bioinformatics* 2008, **9**:559.
36. Shannon P, Markiel A, Ozier O, Baliga NS, Wang JT, Ramage D, Amin N, Schwikowski B, Ideker T: **Cytoscape: a software environment for integrated models of biomolecular interaction networks**. *Genome Res* 2003, **13**(11):2498-2504.
37. Chin CH, Chen SH, Wu HH, Ho CW, Ko MT, Lin CY: **cytoHubba: identifying hub objects and sub-networks from complex interactome**. *BMC Syst Biol* 2014, **8 Suppl 4**(Suppl 4):S11.
38. Jiang T, Zhang M, Wen C, Xie X, Tian W, Wen S, Lu R, Liu L: **Integrated metabolomic and transcriptomic analysis of the anthocyanin regulatory networks in Salvia miltiorrhiza Bge. flowers**. *BMC Plant Biol* 2020, **20**(1):349.
39. Livak KJ, Schmittgen TD: **Analysis of relative gene expression data using real-time quantitative PCR and the 2(-Delta Delta C(T)) Method**. *Methods* 2001, **25**(4):402-408.
40. Singh VK, Mangalam AK, Dwivedi S, Naik S: **Primer Premier: Program for Design of Degenerate Primers from a Protein Sequence**. *BioTechniques* 1998, **24**(2):318-319.
41. Kanehisa M, Goto S: **KEGG: kyoto encyclopedia of genes and genomes**. *Nucleic Acids Res* 2000, **28**(1):27-30.
42. Bechtel W: **Hierarchy and levels: analysing networks to study mechanisms in molecular biology**. *Philos Trans R Soc Lond B Biol Sci* 2020, **375**(1796):20190320.
43. Balfagón D, Pascual LS, Sengupta S, Halliday KJ, Gómez-Cadenas A, Peláez-Vico M, Sinha R, Mittler R, Zandalinas SI: **WRKY48 negatively regulates plant acclimation to a combination of high light and heat stress**. *Plant J* 2024, **117**(6):1642-1655.
44. Zhao PX, Zhang J, Chen SY, Wu J, Xia JQ, Sun LQ, Ma SS, Xiang CB: **Arabidopsis MADS-box factor AGL16 is a negative regulator of plant response to salt stress by downregulating salt-responsive genes**. *New Phytol* 2021, **232**(6):2418-2439.
45. Chen X, Liu J, Lin G, Wang A, Wang Z, Lu G: **Overexpression of AtWRKY28 and AtWRKY75 in Arabidopsis enhances resistance to oxalic acid and Sclerotinia sclerotiorum**. *Plant Cell Reports* 2013, **32**(10):1589-1599.
46. Guyer D, Patton D, Ward E: **Evidence for cross-pathway regulation of metabolic gene expression in plants**. *Proceedings of the National Academy of Sciences* 1995, **92**(11):4997-5000.
47. Giné-Bordonaba J, Busatto N, Larrigaudière C, Lindo-García V, Echeverria G, Vrhovsek U, Farneti B, Biasioli F, De Quattro C, Rossato M *et al*: **Investigation of the transcriptomic and metabolic changes associated with superficial scald physiology impaired by lovastatin and 1-methylcyclopropene in pear fruit (cv. "Blanquilla")**. *Horticulture Research* 2020, **7**(1):49.
48. Hu Y, Tian C, Song S, Li R: **Insights on the enhancement of chilling tolerance in Rice through over-expression and knock-out studies of OsRBCS3**. *Plant Signaling & Behavior* 2024, **19**(1):2318514.

49. Xu Z, Wang M, Xu D, Xia Z: **The Arabidopsis APR2 positively regulates cadmium tolerance through glutathione-dependent pathway**. *Ecotoxicol Environ Saf* 2020, **187**:109819.
50. Wang M, Zhu X, Huang Z, Chen M, Xu P, Liao S, Zhao Y, Gao Y, He J, Luo Y *et al*: **Controlling diurnal flower-opening time by manipulating the jasmonate pathway accelerates development of indica-japonica hybrid rice breeding**. *Plant Biotechnol J* 2024.
51. Bechtold U, Penfold CA, Jenkins DJ, Legaie R, Moore JD, Lawson T, Matthews JSA, Vialet-Chabrand SRM, Baxter L, Subramaniam S *et al*: **Time-Series Transcriptomics Reveals That AGAMOUS-LIKE22 Affects Primary Metabolism and Developmental Processes in Drought-Stressed Arabidopsis**. *The Plant Cell* 2016, **28**(2):345-366.
52. Zhao Y, Jia K, Tian Y, Han K, El-Kassaby YA, Yang H, Si H, Sun Y, Li Y: **Time-course transcriptomics analysis reveals key responses of populus to salt stress**. *Industrial Crops and Products* 2023, **194**:116278.
53. Wang X, Wu Y, Sun M, Wei X, Huo H, Yu L, Zhang J: **Dynamic transcriptome profiling revealed key genes and pathways associated with cold stress in castor (Ricinus communis L.)**. *Industrial Crops and Products* 2022, **178**:114610.
54. Upadhyay A, Gaonkar T, Upadhyay AK, Jogaiah S, Shinde MP, Kadoo NY, Gupta VS: **Global transcriptome analysis of grapevine (Vitis vinifera L.) leaves under salt stress reveals differential response at early and late stages of stress in table grape cv. Thompson Seedless**. *Plant Physiology and Biochemistry* 2018, **129**:168-179.
55. Rather GA, Sharma A, Jeelani SM, Misra P, Kaul V, Lattoo SK: **Metabolic and transcriptional analyses in response to potent inhibitors establish MEP pathway as major route for camptothecin biosynthesis in Nothapodytes nimmoniana (Graham) Mabb**. *BMC Plant Biol* 2019, **19**(1):301.
56. Chen H, Lai Z, Shi J, Xiao Y, Chen Z, Xu X: **Roles of arabidopsis WRKY18, WRKY40 and WRKY60 transcription factors in plant responses to abscisic acid and abiotic stress**. *BMC Plant Biology* 2010, **10**(1):281.
57. Li J, Besseau S, Törönen P, Sipari N, Kollist H, Holm L, Palva ET: **Defense-related transcription factors WRKY70 and WRKY54 modulate osmotic stress tolerance by regulating stomatal aperture in Arabidopsis**. *New Phytol* 2013, **200**(2):457-472.
58. Shen Z, Yao J, Sun J, Chang L, Wang S, Ding M, Qian Z, Zhang H, Zhao N, Sa G *et al*: **Populus euphratica HSF binds the promoter of WRKY1 to enhance salt tolerance**. *Plant Science* 2015, **235**:89-100.

Figures

Fig.1

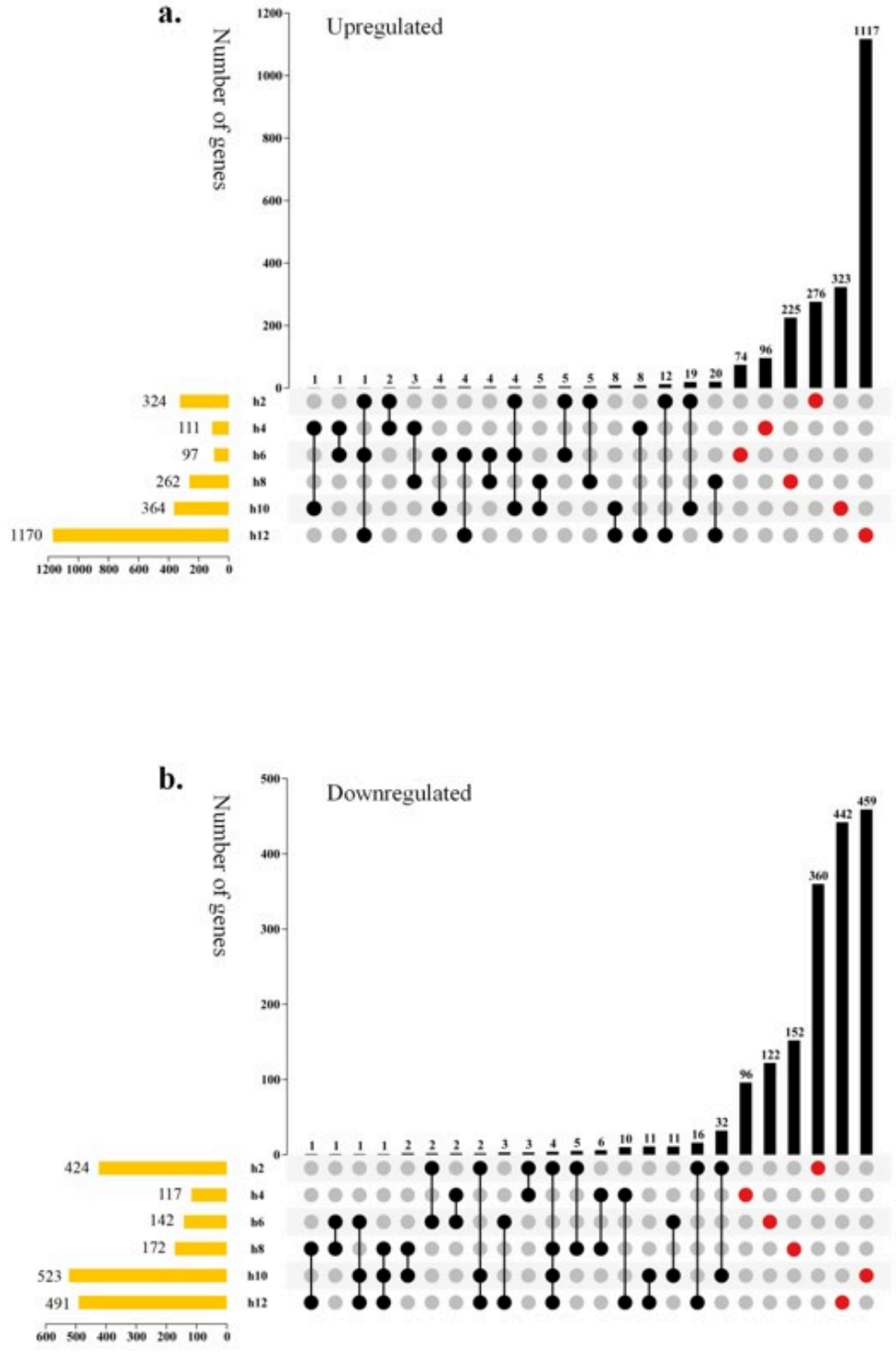


Figure 1

The DEGs at different time points. a. upset plot shows the number of up-regulated DEGs ; b. upset plot shows the number of down-regulated DEGs. The upper part of the bar graph indicates the expression pattern of DEGs at different time points, and the total number of genes up-regulated and down-regulated at each time point is shown on the left side. “h2”, “h4”, “h6”, “h8”, “h10”, and “h12” indicate that the samples were collected after LOV treatment for 2, 4, 6, 8, 10, and 12 hours.

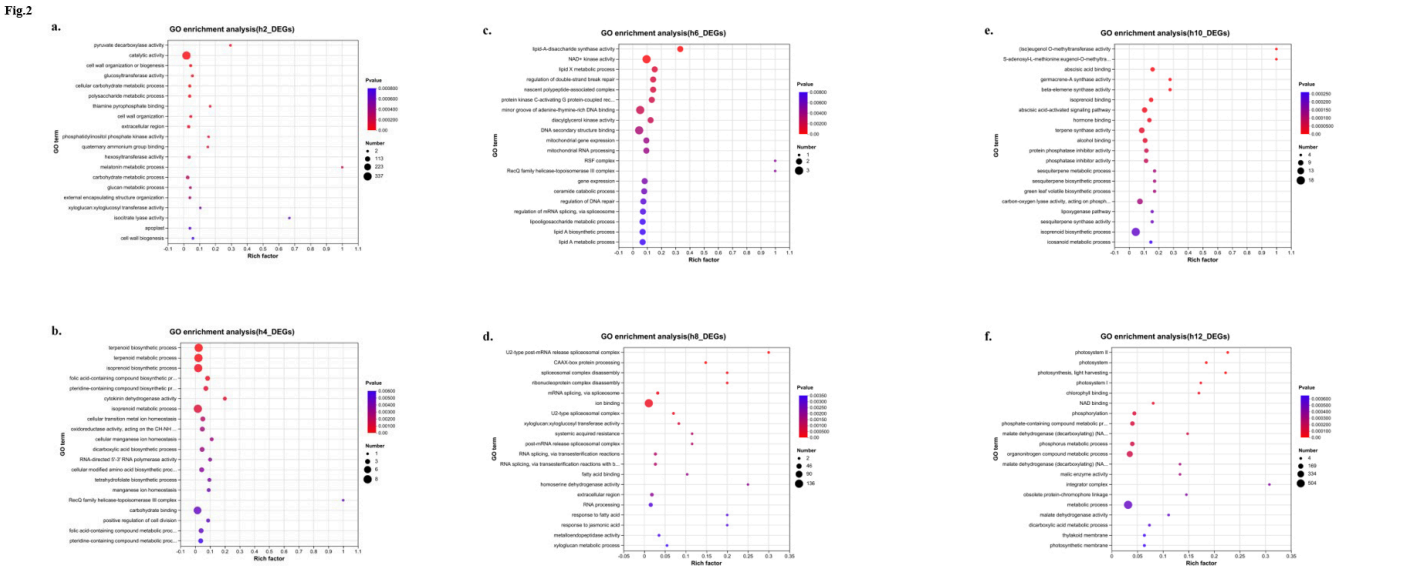


Figure 2

Bubble plots of GO enrichment for DEGs at different times. a-f. Top 20 significantly enriched GO terms at 2, 4, 6, 8, 10, and 12 h.

Fig.3

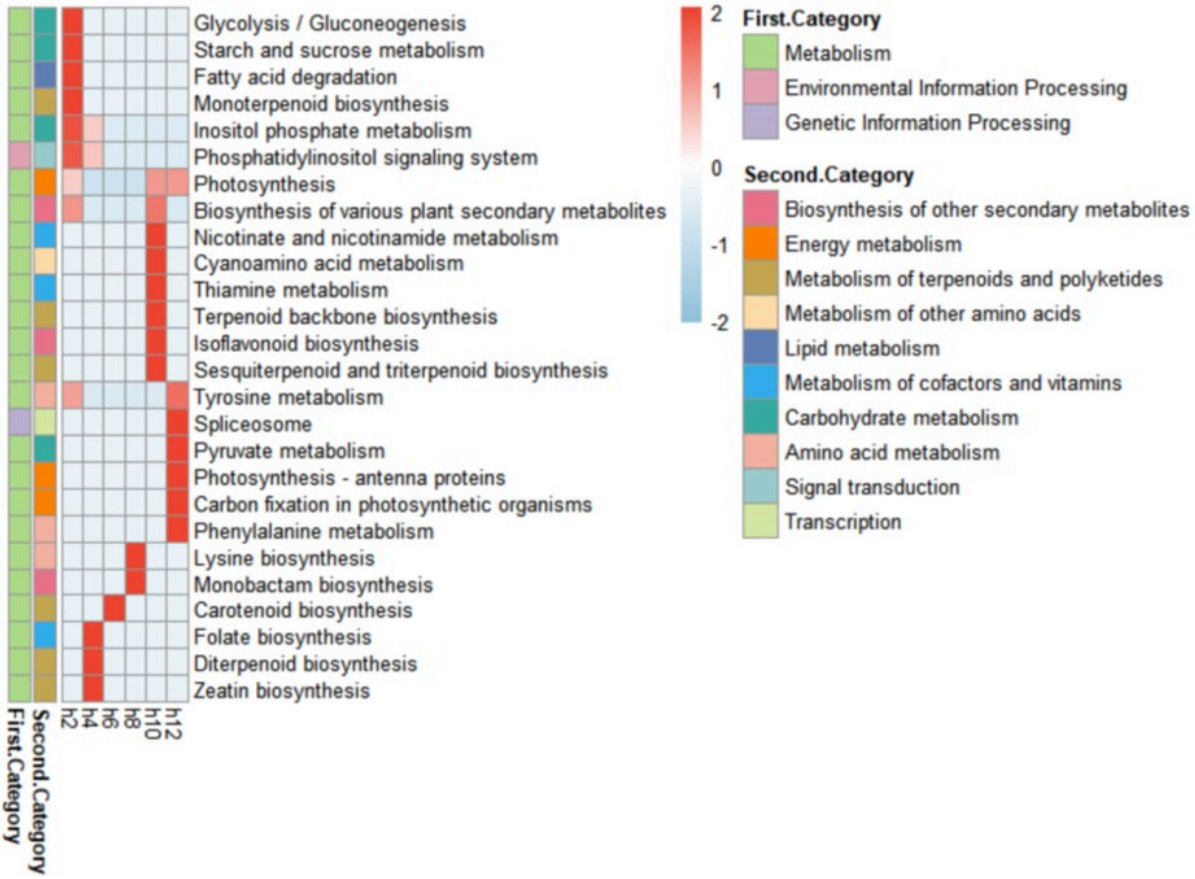


Figure 3

KEGG pathways significantly enriched in DEGs at different time points. Heatmap based on the number of DEGs enriched in each pathway at different times.

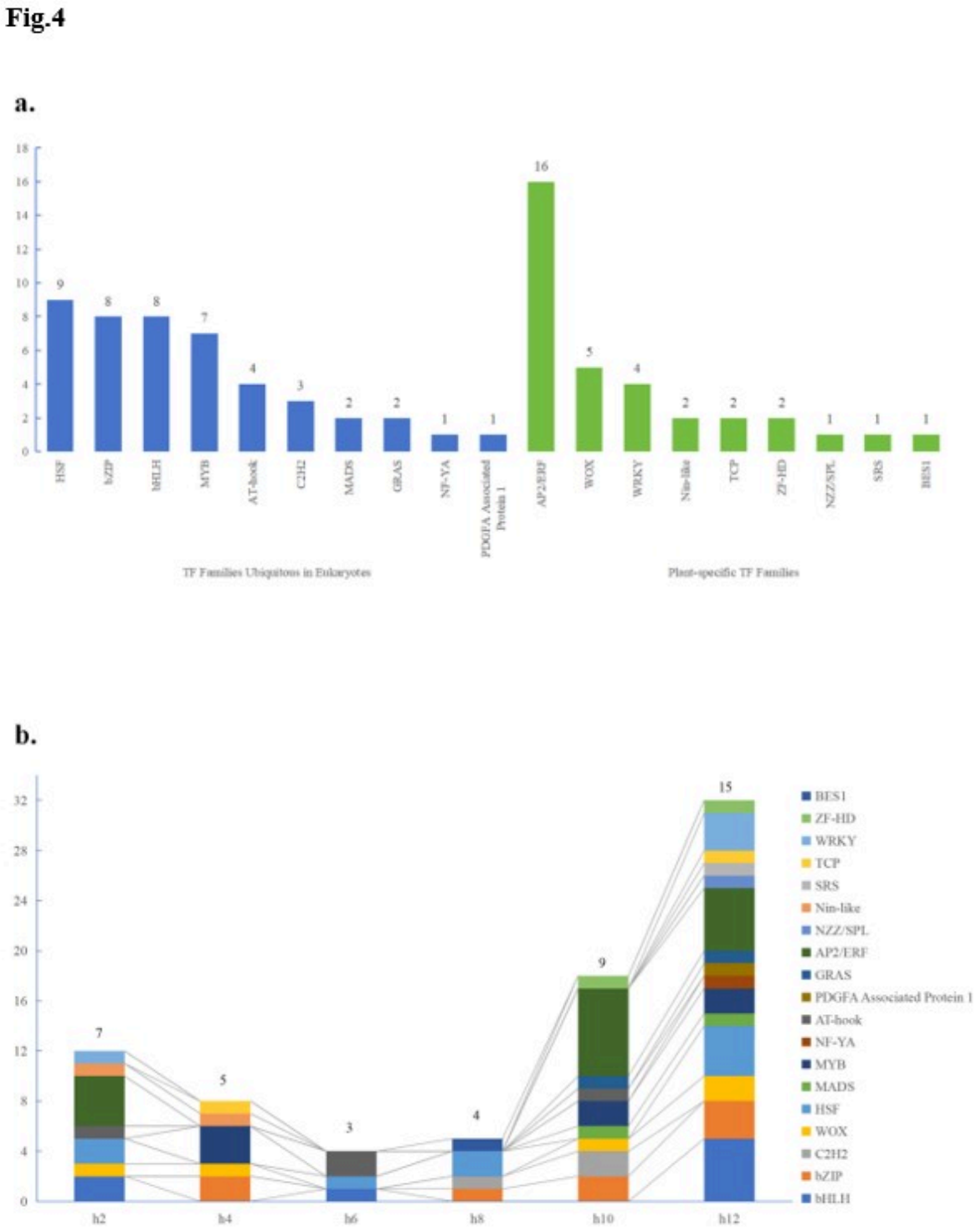


Figure 4

The differentially expressed TFs at each time point. a. Statistics of the number of differentially expressed TFs, the height of the bar indicates the number of members in the transcription factor family, the blue bar indicates the transcription factor families prevalent in eukaryotes, and the green bar indicates the

transcription factor families specific to plants; b. Changes of differentially expressed transcription factor families at different time points, the height of the bar indicates the number of TFs, and the number above indicates the number of transcription factor families.

Fig.5

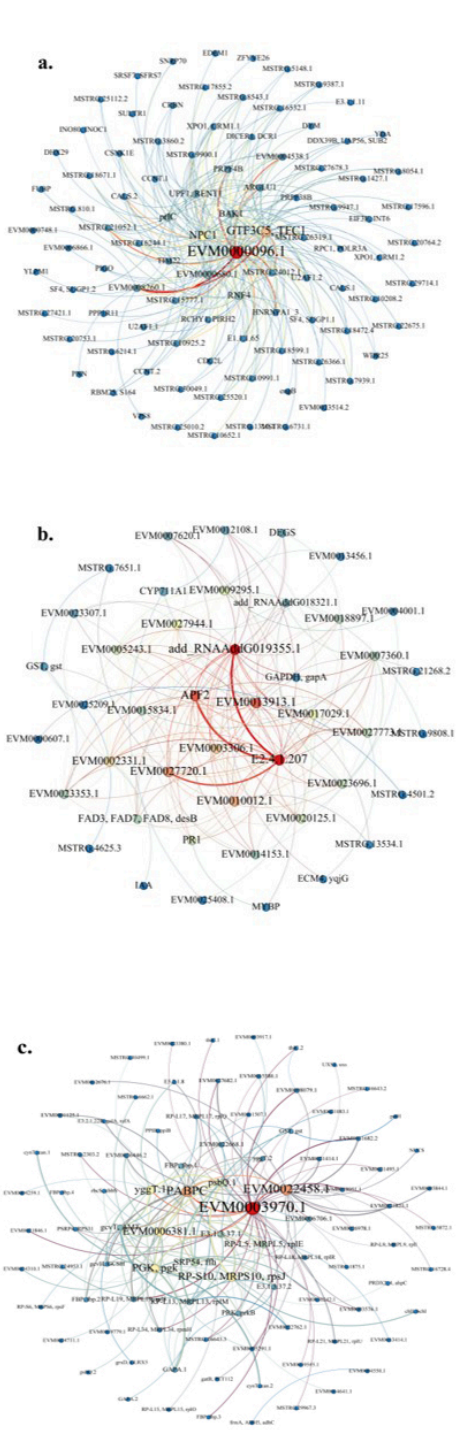


Figure 5

Co-expression network which were constructed based on the genes of the turquoise (a), steel blue (b), and salmon (c) modules. The central genes in the network are indicated by red colour, and the bigger the

node, the higher the centrality.

Fig.6

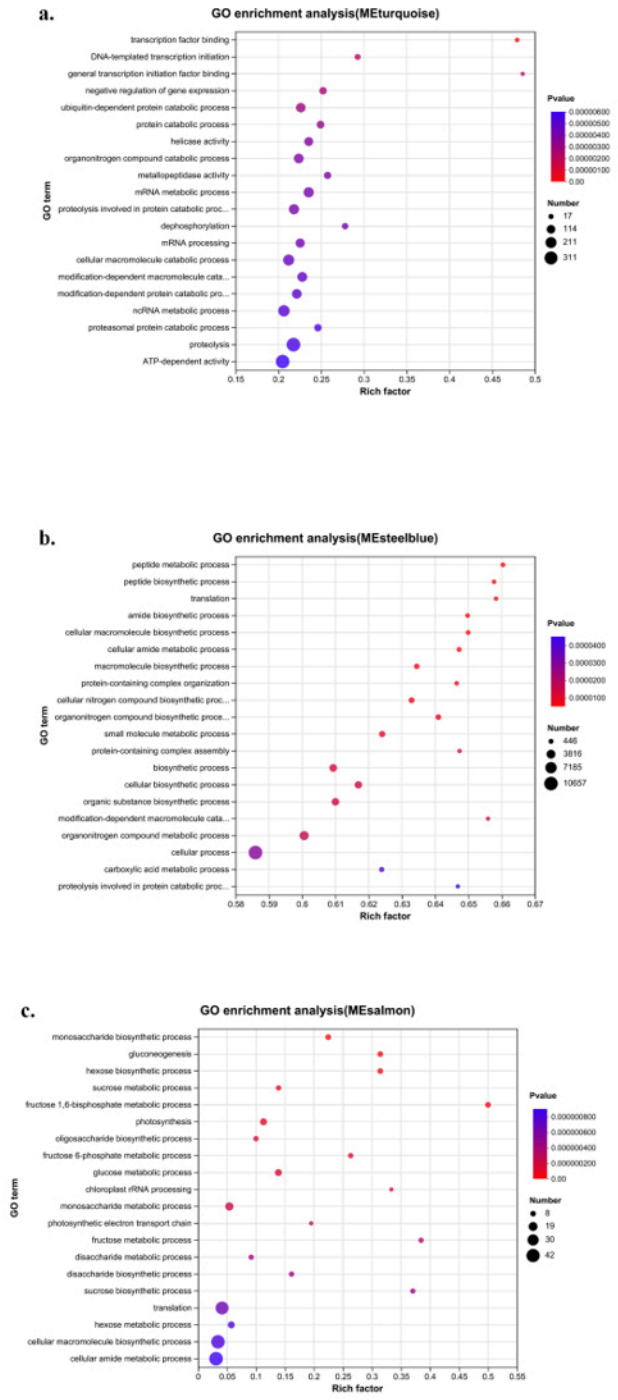


Figure 6

The top 20 significantly enriched GO terms in turquoise (a), steel blue (b), and salmon (c) module.

Fig.7

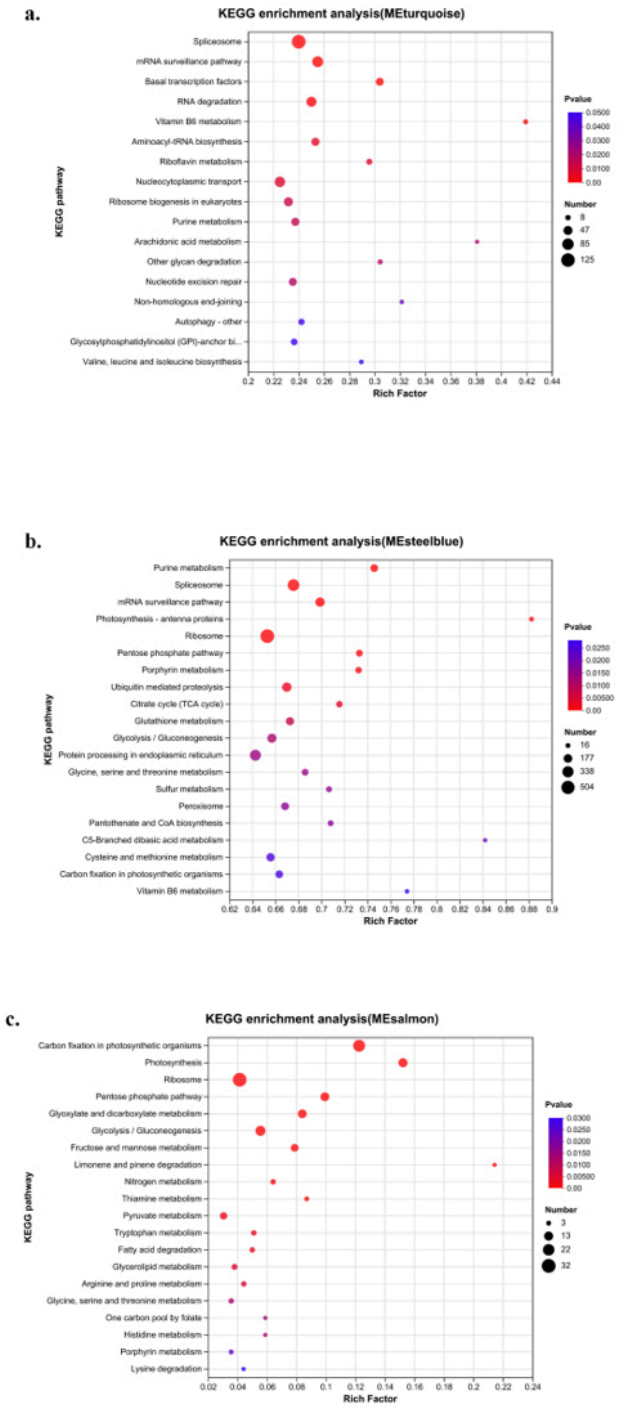


Figure 7

The top 20 significantly enriched KEGG pathways in turquoise (a), steel blue (b), and salmon (c) module.

Fig.8

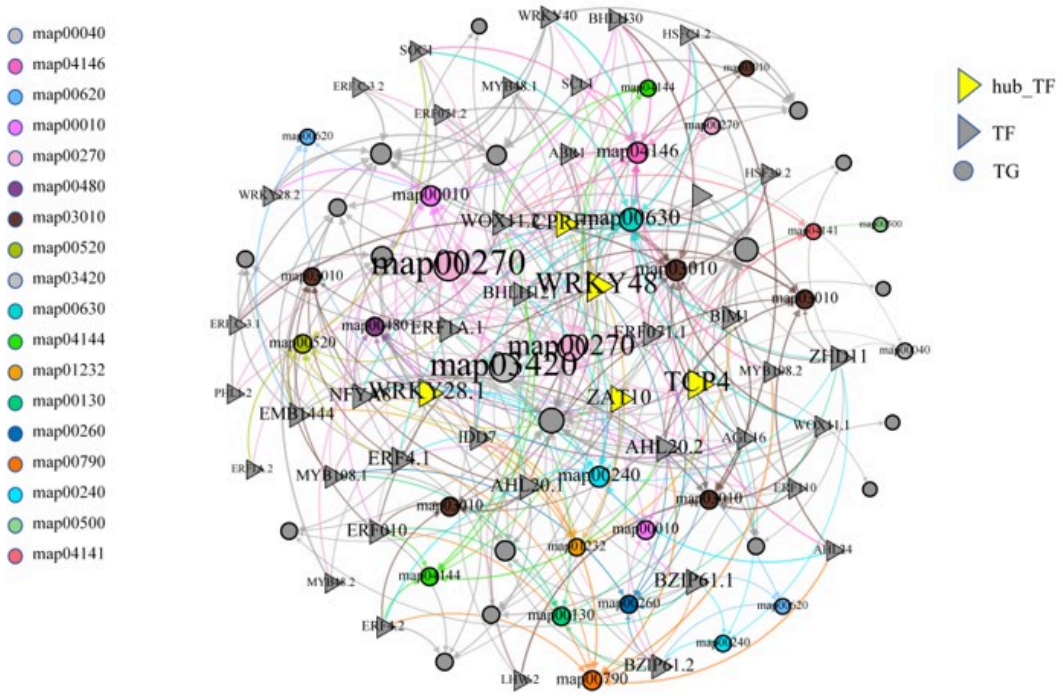


Figure 8

GRNs constructed based on differentially expressed TFs and DEGs of cytoplasmic lysosomal gene sets. ▲: denoting the regulating factors (TFs),●: denoting the target genes (DEGs); ▲(highlighted): denoting hub TFs, ●(different colours): denoting DEGs in different biological pathways.

Fig.9

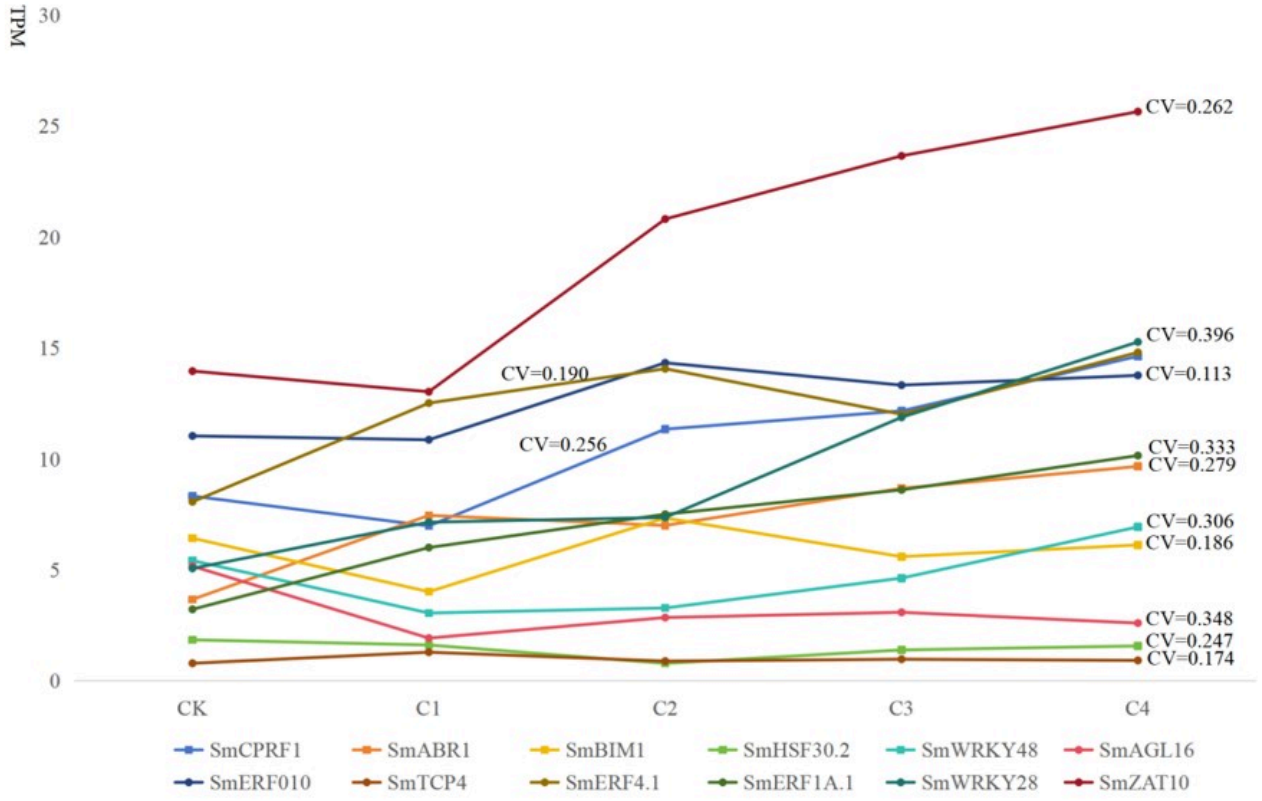


Figure 9

Expression profiles of hub genes of five GRNs after treatment with different concentrations of LOV. CK: control; C1-C4: samples which were collected from MS medium containing the LOV final working solution concentrations of 10 μM, 50 μM, 100 μM, and 200 μM; CV: coefficient of variation.

Fig.10

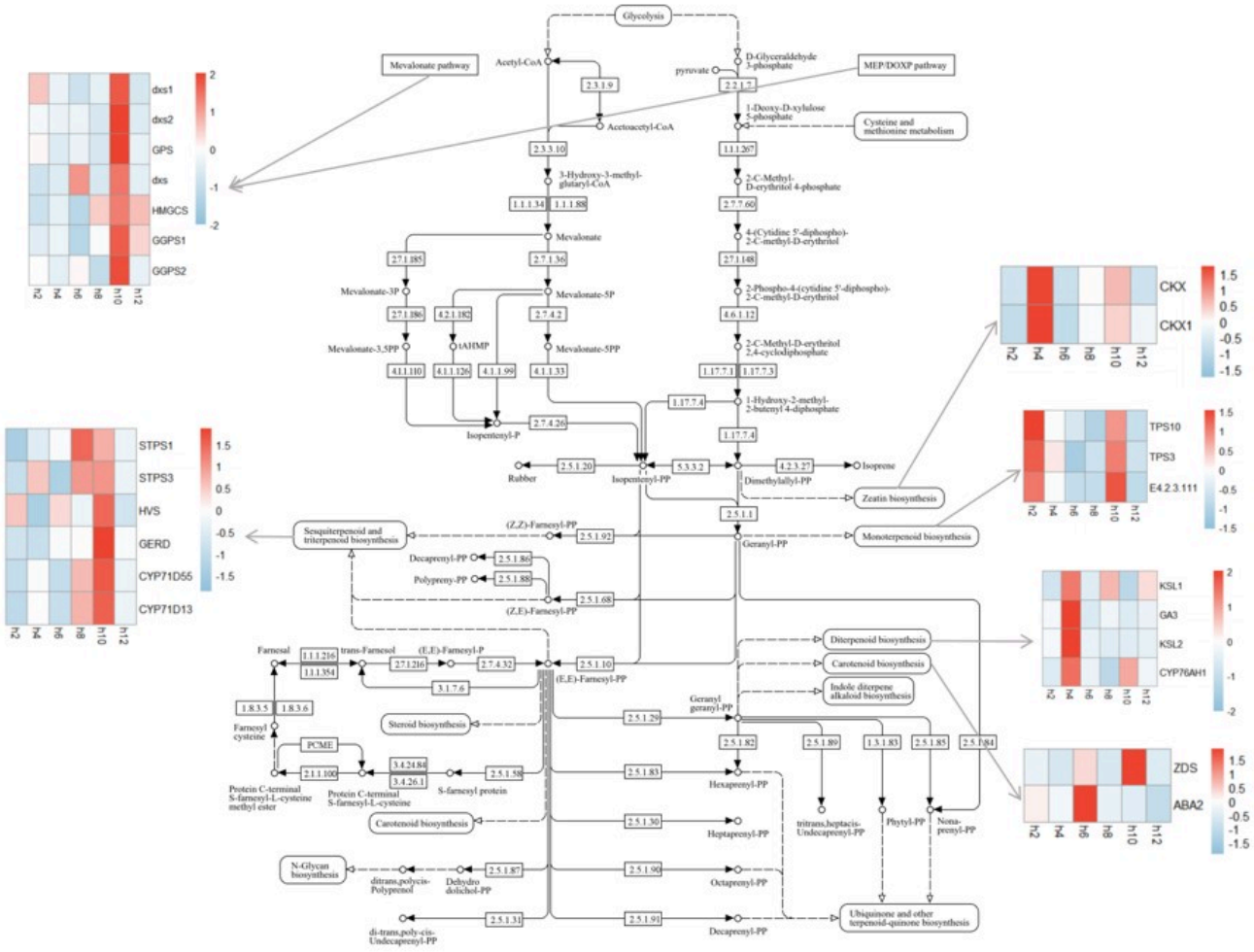


Figure 10

Diagram of terpenoid backbone biosynthesis pathways (taken from KEGG website http://www.genome.jp/kegg). The heatmap shows the |log2 (fold change)| value of differentially expressed genes in different terpenoid biosynthesis pathways. The locations marked by heatmap in the figure are the pathways significantly enriched for differentially expressed genes at different time points.

Supplementary Files

This is a list of supplementary files associated with this preprint. Click to download.

- SupplementaryTables.zip
- SupplyFig.docx